Appl. Phys. B 68, 439–445 (1999)

**Applied Physics B**
Lasers
and Optics


# Time-resolved two-photon photoemission spectroscopy of HOPG and Ag nanoparticles on HOPG

**K. Ertel, U. Kohl, J. Lehmann, M. Merschdorf, W. Pfeiffer, A. Thon, S. Voll, G. Gerber**

Physikalisches Institut, Universität Würzburg, D-97074 Würzburg, Germany
(Fax: +49-931/888-4906, E-mail: pfeiffer@physik.uni-wuerzburg.de)

Received: 6 November 1998

**Abstract.** Time-resolved two-color two-photon photoemission experiments are used to investigate the electronic dynamics in highly oriented pyrolytic graphite (HOPG) and in Ag nanoparticles grown on HOPG. The multiphoton photoemission using 267 nm and 400 nm excitation is presented and discussed. For the first time the known unoccupied state on graphite 3.6 eV above the Fermi level can be identified as an image potential state. A lower limit of 60 fs is given for the lifetime of this state. The two-color experiments reveal that the carrier relaxation deduced from time-resolved experiments is influenced by feeding of the intermediate states. First results of the strongly enhanced multiphoton photoemission from Ag nanoparticles on HOPG at 400 nm wavelength are presented. This observation is explained by the excitation of the surface plasmon and its subsequent decay.

**PACS:** 78.47.+p; 79.60.Jv; 79.60.-i; 82.65.Jv

Graphite and metallic nanoparticles grown on graphite are very interesting systems for nonlinear optical studies using two-photon photoemission spectroscopy (2PPES) and its time-resolved counterpart. The electron dynamics of the pure graphite surface show distinct differences to that of a three-dimensional electron gas system like bulk metals, which have already been thoroughly investigated by time-resolved 2PPES [1–4]. The interpretation of time-resolved 2PPES results by Xu et al. [5] has recently initiated a controversy concerning the hot carrier relaxation mechanisms in graphite. The authors explain the observed deviation from standard Fermi liquid theory [6] by an additional plasmon mediated relaxation mechanism. However, this interpretation has been questioned [7] and the debate is still going on. Experimental evidence like the two-color time-resolved 2PPES experiments presented here provides further substantial information.

Another important issue is related to the study of the unoccupied states of graphite. With the development of inverse photoemission spectroscopy (IPES) and target current spectroscopy (TCS) the unoccupied states of graphite were investigated [8–10]. Good agreement with theory was found for most of the observed states [11]. However, the assignment of one state about 3.6 eV above the Fermi level remained doubtful [10]. From the observation that this state disappears in the presence of adsorbates it was deduced that it is most likely a surface state; nonetheless it remained impossible to distinguish between an image potential state and an intrinsic surface state on the basis of the available data [10]. Time-resolved 2PPES is well suited to gain additional information to identify its nature.

Well-defined metal nanoparticles grown on clean surfaces under UHV conditions are ideal for investigating heterogeneous catalysis and are therefore widely used as model catalysts [12]. As in most surface reactions the dynamic electronic properties of these nanoparticles, especially the relaxation of hot carriers, determine their catalytic properties. Furthermore, the coupling between nanoparticle and substrate is relevant, but only poorly understood. Compared to the homogeneous surface, the investigation of the electronic dynamics of a heterogeneous system is complicated due to the different signal contributions from its components. However, if this problem is solved, the application of time-resolved 2PPES gives insight into the catalytic mechanism.

In this paper we present first results of 2PPES and time-resolved 2PPES measurements of highly oriented pyrolytic graphite (HOPG) covered with Ag nanoparticles. The choice of this model system was guided by the facts that (i) HOPG is a conducting material with a fairly inert surface, (ii) Ag nanoparticles exhibit a strong surface plasmon resonance close to 400 nm [13, 14], which can be excited by the second harmonic of the employed femtosecond Ti:sapphire laser, and (iii) the preparation of homogeneously distributed Ag nanoparticles with a narrow size distribution has recently been demonstrated [15]. The excitation of the surface plasmon is of special interest since recent theoretical work has shown that the decay of the surface plasmon via direct photoemission is an important damping mechanism [16]. To our knowledge there exists only one other study that investigates the electronic properties of Ag clusters on HOPG using time-resolved 2PPES [17]. In that case, the size of the Ag clusters was in the range of up to 9 atoms, whereas we present results on Ag nanoparticles of about 5 nm diameter.

In the following we give a short survey of the experiment. The analysis of the single-photon and multiphoton photoemission spectra obtained with 400 nm and 267 nm on the pure HOPG surface allows us to identify all observed spectral features. We then present time-resolved 2PPES results on the hot carrier relaxation and the properties of the surface state. On the basis of the observed long lifetime of the surface state we identify it as an image potential state. Finally we present first results of 2PPES and time-resolved 2PPES of Ag nanoparticles grown on HOPG.

## 1 Experiment

The HOPG samples [18] are cleaved under ambient conditions immediately before transfer into the UHV load-lock chamber. After heating the sample (30 min, 300 °C) the tunneling junction of the UHV-STM is usually stable and the STM topography shows no significant traces of surface contamination. The preparation of the Ag nanoparticles on HOPG follows the procedure described by Hövel et al. [15]. After slightly damaging the HOPG surface by a very gentle sputter process ($Ar^+$, 1 keV, 1 nA cm$^{-2}$, 20 s), the sample is oxidized for 20 min at 530 °C under air. At this temperature the oxidation occurs at the Ar-ion-induced defects, leading to the formation of etch pits on the HOPG surface. Ag is evaporated at 350 °C sample temperature onto this surface (0.1 Å s$^{-1}$, 10 s) and is mobile on HOPG, but is trapped at the small etch pits and at Ag nanoparticles. This leads to a continuous growth of the Ag nanoparticles that are attached to the etch pits. Due to this growth mechanism the density of nanoparticles is controlled by the etch pit density whereas the average Ag coverage determines the size of the particles. Since the Ag nanoparticles are pinned at the etch pits it is possible to obtain stable STM topographies even at room temperature. A typical STM topography of an Ag nanoparticle is shown in Fig. 1. The height of the nanoparticles of 2.5 nm can be unambiguously determined from the STM image, whereas the lateral extension of the cluster is difficult to determine due to the convolution of the actual cluster shape and the unknown tip shape. For Au nanoparticles on HOPG the ratio of cluster height to width is known to be 0.7 from the comparison of transmission electron microscopy and STM results [15]. Assuming a similar axial ratio for Ag particles a lateral width of the cluster shown in Fig. 1 of about 5 nm can be estimated. From this and the density of the nanoparticles on HOPG we determine that about 2% of the HOPG surface is covered by Ag nanoparticles. Besides the growth of Ag nanoparticles in the etch pits some Ag nanoparticles are also formed along steps on the HOPG surface. These particles are no longer well separated and homogeneously distributed but form an almost connected chain. From STM topographies of larger areas of the sample we estimate that about 50% of the nanoparticles are located in individual etch pits. The average distance between these particles is about 50 nm.

In our experiments we employed a self-built Ti:sapphire laser system. The stretched output of the femtosecond oscillator (80 MHz, 4 nJ, 45 fs, 800 nm) seeds a high repetition rate regenerative amplifier. The amplified laser pulses are compressed and pulses of 65 fs duration and 2–3 μJ energy are obtained at a repetition rate of up to 300 kHz. In Fig. 2 the

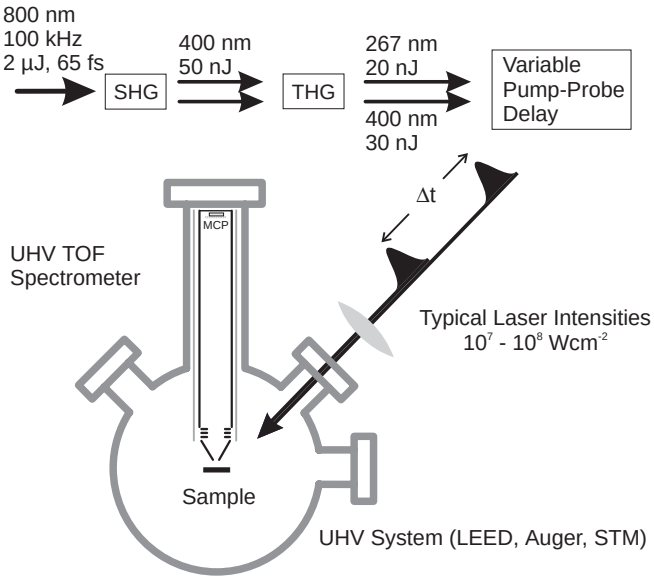


**Fig. 2.** Schematic representation of the experimental setup

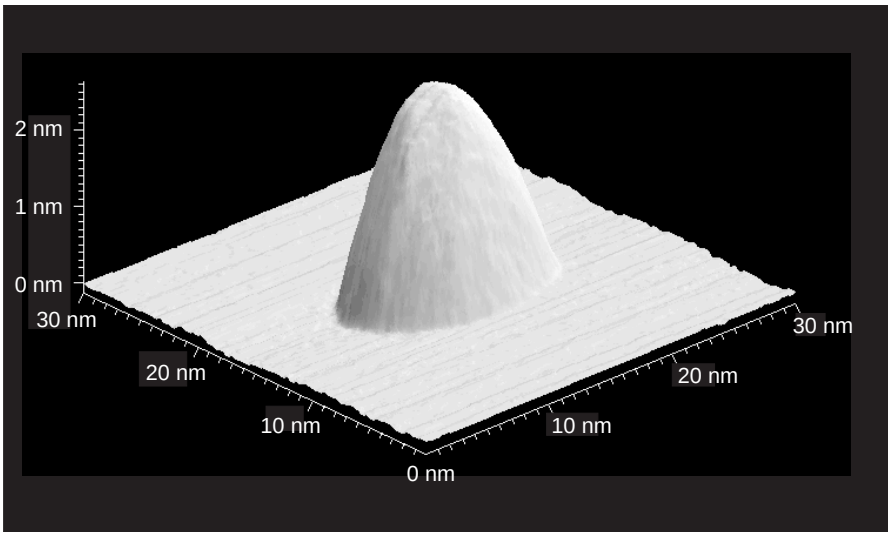


**Fig. 1.** STM image of an Ag nanoparticle on HOPG under UHV condition ($2 \times 10^{-10}$ mbar). The image was recorded at 0.3 V sample bias and 30 pA tunneling current

experimental setup used is schematically displayed. Second harmonic generation of the fundamental wavelength and sum frequency generation with the fundamental and the second harmonic light in two 100 μm thick BBO crystals are used to obtain laser pulses at 400 nm and 267 nm wavelength. The energy per pulse for both wavelengths is 20–30 nJ. Pump and probe pulses with variable time delay are generated by use of a Mach–Zehnder interferometer. Two different prism compressors compensate the material induced chirp.

The photoemission spectra are measured with a self-built UHV time-of-flight (TOF) spectrometer. In order to reduce the influence of stray fields a small extraction voltage of 5 V is applied between sample and spectrometer. The arrival time of the individual electrons is detected by a fast multichannel plate detector (MCP) in combination with a time-to-amplitude converter (TAC). Laser intensities are usually attenuated to $10^7$–$10^8$ Wcm$^{-2}$ so that the probability of detecting one photoelectron per laser pulse is below 0.1. The energy calibration of the TOF spectra is complicated by the fact that the work function difference $\Delta W$ between sample and spectrometer is unknown. We estimate $\Delta W$ from the comparison of the calculated time-of-flight for photoelectrons with zero kinetic energy with the measured one. This allows us to determine the relation between the time-of-flight and electron kinetic energy which is used for the coordinate transformation that is necessary to obtain the energy spectrum. The absolute uncertainty of the energy calibration is about 0.1 eV.

Time-resolved 2PPES requires the energy resolved recording of pump–probe spectra. Since the recording of the complete energy spectrum with every laser pulse is one of the major advantages of the TOF technique, it is also desirable to measure the whole spectrum for a given delay time and then move on to the next delay time. This means that a laser drift during this very slow pump–probe scan can severely distort the observed pump–probe effect. The alternative possibility to record only the events in a narrow TOF window and scan the pump–probe delay repeatedly averages over any slow laser drift, but does not retain the advantages of the TOF method. We have therefore combined both techniques. Before and after the consecutive recording of the whole energy spectra at different pump–probe delays we repeatedly record the integrated electron count rate as a function of the delay. The obtained smooth pump–probe spectra of this electron count rate are later used to correct the individual energy spectra at each pump–probe delay. Tests have shown that pump–probe spectra recorded with this procedure are equivalent to those recorded using narrow TOF windows and that the effects due to laser drift can be corrected.

## 2 Multiphoton photoemission from HOPG

The results of single-photon and multiphoton photoemission from the pure HOPG surface using light of 400 and 267 nm wavelength are displayed in Fig. 3. The lower two spectra are recorded with low laser intensity ($\leq 10^8$ Wcm$^{-2}$), whereas the upper two spectra represent the spectral shape at higher laser intensity ($\geq 10^8$ Wcm$^{-2}$). At low laser intensity the electron spectrum obtained with 267 nm excitation is dominated by single-photon photoemission. In this case the spectrum consists of a narrow peak with an exponential decrease extending to about 0.5 eV kinetic electron energy. With increasing laser intensity a broad spectral contribution is continuously growing. This part of the spectrum scales perfectly with the square of the applied laser intensity indicating a two-photon photoemission process. The presence of single-photon photoemission indicates that the work function of the HOPG surface must be smaller than the photon energy of 4.65 eV. The transition regime between two-photon and single-photon photoemission allows a more accurate determination of the work function with an accuracy of about 0.1 eV. From this we conclude that the work function of the used HOPG is 4.3 eV. This method of determining the work function is susceptible to systematic errors. A slightly higher electron work function of about 4.5 eV was deduced from the linear extrapolation of the slope of the single-photon photoemission spectrum with 267 nm excitation. Both values are smaller than the literature value 4.7 eV for the pure graphite surface [10]. However, since cleaning of the surface by either sputtering or heating did not change its work function, we believe that the observed reduction is not due to adsorbates but is an intrinsic property of the used HOPG material.

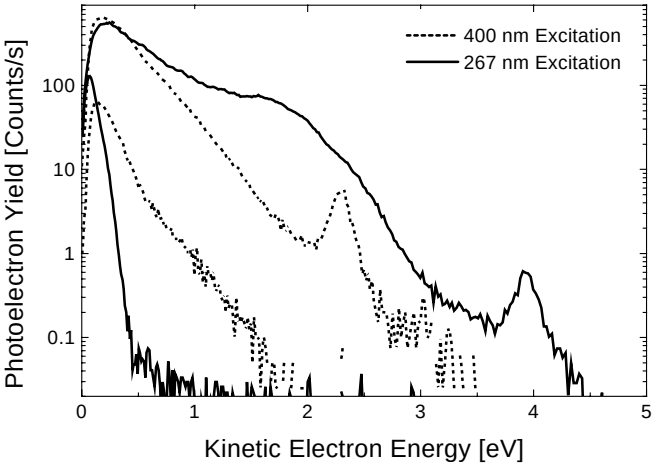


**Fig. 3.** Photoemission spectra of pure HOPG after excitation with 400 nm (*dotted lines*) and 267 nm (*straight lines*). The lower two curves correspond to $10^8$ Wcm$^{-2}$ and $10^6$ Wcm$^{-2}$ for 400 nm and 267 nm wavelength, respectively. The upper two curves were recorded at higher laser intensities, $10^9$ Wcm$^{-2}$ and $10^8$ Wcm$^{-2}$ in the case of 400 nm and 267 nm

The two-photon contribution in the 267 nm spectrum extends to about 4.5 eV kinetic electron energy. Two features are of particular interest. The broad shoulder at about 2 eV kinetic electron energy can be attributed to the high density of initial states in the $\sigma$-band of graphite that is located about 3 eV below the Fermi level. The continuous decrease of occupied states above the $\sigma$-band explains the low photoelectron yield at higher kinetic electron energy. More striking is the presence of a pronounced photoemission peak at 3.9 eV kinetic electron energy. The initial state for this emission is located 1 eV below the Fermi level. Since the density of states has no maximum in this energy regime [11], the enhancement of the emission must result from an intermediate state 3.6 eV above the Fermi level.

At 400 nm excitation wavelength (3.1 eV) and low laser intensity the photoemission occurs via a two-photon process. Again the highest photoelectron yield is observed at low electron energy followed by an exponential decay for increasing kinetic electron energy. The shape of the spectrum can be understood in terms of the vanishing density

of states at the Fermi level in graphite [11]. The exponential shape of the spectrum makes it difficult to determine the limit for two-photon photoemission. By comparing spectra at different laser intensity we can locate this limit at about 2 eV. This is in very good agreement with the work function of 4.3 eV deduced from the single-photon photoemission limit with 267 nm excitation. At higher laser intensity the photoelectron spectrum extends to much higher kinetic electron energies of about 3.3 eV, indicating that higher order multiphoton processes play a role. It is difficult to identify the excitation mechanism for the photoelectrons close to this limit. In contrast this is possible for the additional peak in the photoemission spectrum seen at about 2.3 eV. The photoemission peaks in the spectra with 400 nm and 267 nm excitation are separated by 1.6 eV. Within the experimental uncertainty this is exactly the energy of the fundamental wavelength of the laser system (800 nm, 1.55 eV). This indicates that in both spectra the last step of the multiphoton process starts from the same intermediate state 3.6 eV above the Fermi level. Accordingly, with 400 nm excitation wavelength this state is populated by a two-photon process and a third photon is required for the photoemission.

The energy diagram for the different multiphoton excitation processes of HOPG is shown in Fig. 4. Summarizing, we find that the observed multiphoton photoemission spectra obtained at 400 nm and 267 nm are consistent with the known bulk band structure of graphite [11]. The resonant intermediate state requires some further discussion. The presence of an unoccupied state about 4 eV above the Fermi level is known already from work of Fauster et al. [8]. However, the identification of the physical nature of this state remained controversial. Initially it was assigned to the unoccupied antibonding $\sigma$-band [8, 19], but later it was suggested to be a surface state [10]. The surface state assignment is in good agreement with our observation that the relative strength of the photoemission peak decreases over time and is influenced by the surface preparation. Theory predicts an unoccupied intrinsic surface state at 3.8 eV above the Fermi level split off from the interlayer band [20]. Experimental evidence to decide between this explanation and the alternative explanation of an image potential state proposed by Schäfer et al. [9] has so far still been lacking. The time-resolved 2PPES results presented in the next paragraph provide this missing information.

## 3 Time-resolved two-photon photoemission spectroscopy of pure HOPG

On the basis of the known excitation pathways in multiphoton photoemission on HOPG with 267 nm and 400 nm light, the results of two-color pump–probe experiments can now be analyzed. The surface state can be populated by the 267 nm pump pulse and the population in this state is then photoemitted by the 400 nm probe pulse. The corresponding photoelectrons appear at the same energy as the photoemission peak in the spectrum taken with high intensity 400 nm excitation (Fig. 3). A pump–probe spectrum recorded at this electron energy is shown in Fig. 5 together with a spectrum recorded at 0.3 eV lower kinetic electron energy. The latter spectrum is symmetric with respect to zero delay time. In contrast, the pump–probe effect on the surface state is asymmetric and its maximum is shifted relative to zero delay time by 40 fs. The shift towards positive delay confirms that the 267 nm pulse acts as pump pulse. Both observations, shift and asymmetry, clearly indicate that the intermediate state has a significant lifetime compared to the pulse duration. In order to extract more quantitative information we have used the optical Bloch equations for a two level system to fit the experimental data following the procedure described by Hertel et al. [21]. Since we have no independent measurement of the cross correlation of the laser pulses used, we used the pump–probe spectrum 0.3 eV below the surface state as an estimate for the cross correlation width and assumed equal pulse duration of 95 fs for pump and probe pulse. From the linewidth of 0.18 eV obtained from a Lorentzian fit of the photoemission peak, one can deduce a lower limit for the dephasing time $T_2$ of 7 fs. The best fit to the pump–probe spectrum of the surface state was achieved with a lifetime of $60 \pm 5$ fs and the lower limit of the dephasing time $T_2$. The fit neither follows the rising nor the falling slope of the pump–probe signal perfectly. This

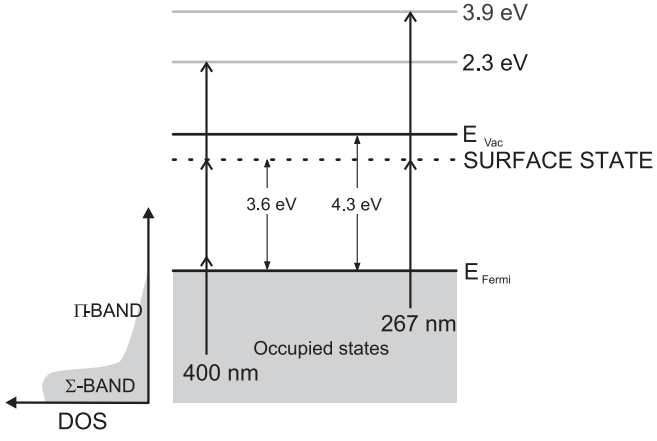


**Fig. 4.** Schematic representation of the multiphoton excitation of the surface state on HOPG with light of 267 nm and 400 nm wavelength. On the left the schematic density of occupied states for graphite is shown

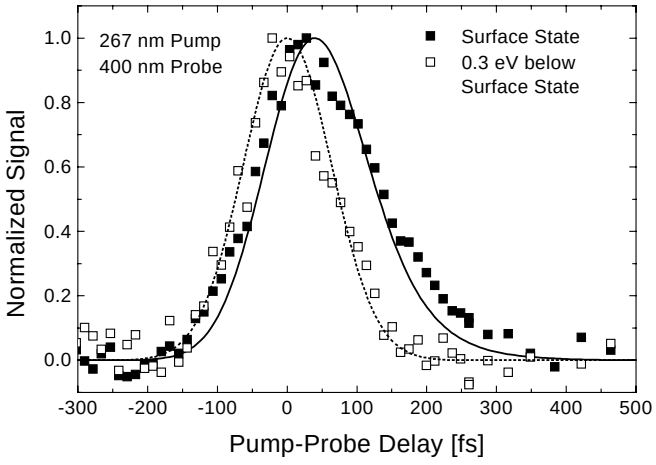


**Fig. 5.** Normalized pump–probe spectra for two-photon photoemission via the surface state (*closed symbols*) and via a level 0.3 eV below the surface state (*open symbols*) are shown. The spectral width for the pump–probe spectra is 0.1 eV. The optical Bloch equations for a two level system were used to fit the experimental data (*continuous curves*)

could be due to the large uncertainty in the determination of the pulse duration and the assumption of equal pulse duration for pump and probe pulse. An exponential fit to the tail of the pump–probe signal at positive delay times at which pump and probe pulse no longer overlap reveals a lifetime of $100 \pm 10$ fs. A more detailed study of the properties of the surface state is in preparation and will be published elsewhere [22]. However, a lifetime of the surface state in the range of 60 fs or even longer is obvious from the pump–probe signal. Such long lifetimes are unknown for intrinsic surface states. From this we conclude that the observed surface state cannot be an intrinsic surface state but must be an image potential state. This is also in good agreement with the location 0.7 eV below the vacuum level [23]. Preliminary results reveal an additional intermediate state at about 4 eV above the Fermi level. This singular observation nicely corresponds to the $n = 2$ image potential state and supports the identification given above.

Besides the investigation of the surface state two-color time-resolved 2PPES allows to study the hot carrier relaxation processes in HOPG. Pump–probe spectra at three different kinetic electron energies are displayed in Fig. 6. The slow slope of the pump–probe signal towards negative delay times implies that the corresponding process is due to electrons that are pumped by the 400 nm pulse. Therefore the slope at negative delay corresponds to the occupation of intermediate states 0.7 eV, 0.4 eV and 0.2 eV above the Fermi level. As expected, the energy relaxation that close to the Fermi level is rather slow.

In the range of temporal overlap of pump and probe pulse a shift of the maximum of the pump–probe signal together with a change of its fast slope is seen. The absence of any significant pump–probe signal at positive delay outside the range of overlap of pump and probe pulse indicates that the energy relaxation in the intermediate states probed by the 400 nm pulse (2.2 eV, 1.9 eV and 1.7 eV above the Fermi level) is either too fast or that these states are populated only to a minor extent by the 267 nm pump pulse. Due to this mixing of two excitation pathways the interpretation of the results in the range of temporal overlap of pump and probe pulse is more complicated. Lifetimes of less than 20 fs can be estimated for the intermediate states probed by 400 nm pulses from the extrapolation of the lifetime as a function of the energy of the intermediate state above the Fermi level given by Xu et al. (Fig. 2 in [5]). Pump–probe signal contributions with such short lifetimes cannot explain the observed change in the fast slope of the pump–probe signal. In addition, the initial state for the 267 nm pump process is located already above the high density of states of the occupied $\sigma$-band in graphite. Therefore we assume that the multiphoton process via 267 nm pump and 400 nm probe pulse contributes only to a minor extent to the photoelectron yield.

Under this simplifying assumption and neglecting any coherent effects it is possible to fit the results using a simple rate equation model that includes only the pump and probe process and a lifetime of the intermediate state. We used the same parameters as for the fit of the pump–probe spectrum of the surface state. The results are shown in Fig. 6 as continuous curves. It turned out to be impossible to obtain satisfying fit results for the whole pump–probe spectrum. This behavior closely resembles the observation described by Hertel et al. [21]. We attribute this to the disregard of the relaxation cascade that leads to feeding of the intermediate state. This process should mainly influence the slow slope of the pump–probe signal, whereas the fast slope should still be dominated by the lifetime of the intermediate state. We have therefore fitted the rate equation model either to the slow (dotted line) or to the fast slope (solid line) of the signal. The results for the obtained lifetime of the intermediate state are summarized in Fig. 7. The lifetimes extracted from the slow slope of the pump–probe spectra as well as the slope of the energy de-

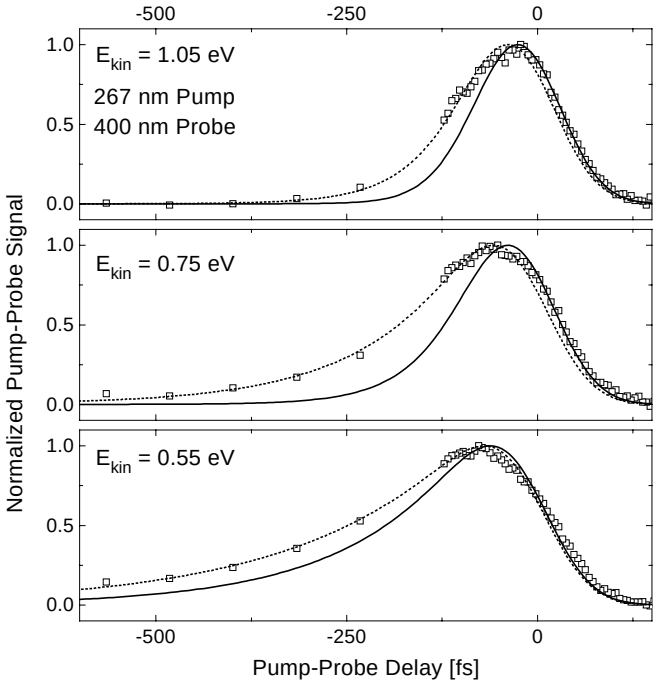


**Fig. 6.** Normalized two-color pump–probe spectra recorded at three different kinetic electron energies (spectral width 0.1 eV). The continuous curves are fit results of a simple rate equation model. The *dotted* and the *solid line* correspond to the best fit to the slow slope ($-700$ fs to $-50$ fs) and to the fast slope (signal maximum to 120 fs), respectively

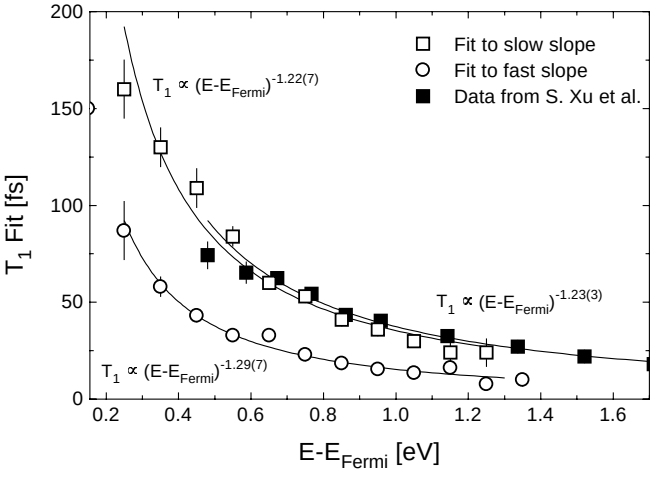


**Fig. 7.** Energy relaxation lifetime $T_1$ as obtained from the fit of a rate equation model to the measured pump–probe spectra is shown as a function of the intermediate state energy. For comparison the data from Xu et al. [5] are also shown. The exponent of the slope of the experimental data was fitted (*continuous curves*)

pendence are in perfect agreement with the results reported by Xu et al. [5]. However, the values corresponding to the fast slope are about two times smaller than those obtained for the slow slope. With the assumptions made above, this means that, under the excitation conditions used, the feeding of intermediate states cannot be excluded as it was done in the paper of Xu et al. [5]. The good agreement for the values obtained from the slow slope can be explained by the fact that these authors have used single-color time-resolved 2PPES that is not able to reveal the presence of feeding processes due to the symmetry of pump and probe pulse. Still, the slopes of the energy relaxation times as a function of the intermediate state energy above the Fermi level for all three data sets (Fig. 7) exhibit an exponent of about $-1.2$. This is significantly lower than the value $-2$ that is expected for a three dimensional free electron gas from standard Fermi liquid theory [6]. Under the assumption that feeding processes can be neglected, Xu et al. [5] have drawn from this observed deviation the conclusion that interlayer plasmon coupling is responsible for the energy relaxation in a layered electron gas system like graphite. This interpretation is questioned by our observation of the presence of feeding processes. Therefore we believe refined experiments at different wavelengths and a more detailed model that takes cascade processes into account are necessary to unambiguously identify the underlying relaxation mechanism in graphite.

## 4 Multiphoton photoemission from Ag nanoparticles

First results of multiphoton photoemission from Ag nanoparticles grown on HOPG are now discussed. The photoemission spectra obtained by excitation with ultrashort pulses at either 400 nm or 267 nm wavelength are shown in Fig. 8. The spectrum due to 267 nm excitation (solid line) consists of a contribution from single-photon photoemission that reaches up to about 0.7 eV kinetic electron energy and another contribution from two-photon photoemission. The ratio between single- and two-photon photoemission from Ag nanoparticles on HOPG is larger compared to pure HOPG (Fig. 3).

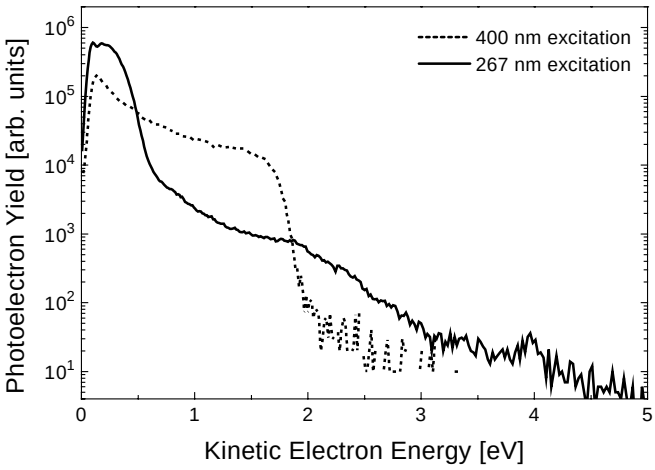


**Fig. 8.** Photoemission spectra from HOPG with Ag nanoparticles on the surface after excitation with laser pulses at 400 nm (*dotted line*) and 267 nm (*solid line*). The laser intensities are $10^7$ Wcm$^{-2}$ (400 nm) and $10^6$ Wcm$^{-2}$ (267 nm). For clarity, the spectrum at 400 nm has been scaled by a factor of 10

The spectral shape of the two-photon contribution, however, closely matches that of pure HOPG. Even the surface state is seen at 4 eV kinetic electron energy. No two-photon photoemission from the Ag nanoparticles can be identified in the spectrum obtained with 267 nm excitation.

A totally different electron spectrum is observed in the case of 400 nm excitation (dotted line in Fig. 8). The spectrum exhibits a clear Fermi edge at the two-photon photoemission limit at 2 eV and the spectral shape closely resembles that of the measured two-photon photoemission spectrum of an Ag crystal surface [24]. The presence of a distinct Fermi edge in the photoelectron spectrum indicates a high density of states at the Fermi level. We can exclude any Ag induced change of the density of states in the HOPG due to the close resemblance of the spectra from pure HOPG and Ag nanoparticles on HOPG at 267 nm excitation. According to this, the photoelectron yield at 400 nm excitation must be dominated by the photoemission from the Ag nanoparticles. The total photoemission yield from the HOPG surface covered with Ag nanoparticles is 50 times higher than that from the HOPG surface with etch pits. Taking into account the low surface coverage of 2% the emission from the Ag nanoparticles is 2000 times stronger than that of the bulk HOPG.

Thus with 267 nm we probe the total surface with no detectable contribution from Ag nanoparticles while with 400 nm strong emission from the Ag nanoparticles is observed. From linear optical spectroscopy of Ag nanoparticles on surfaces and in matrices it is known that the surface plasmon energy is about 3 eV, depending on cluster size, cluster shape and the dielectric constant of the two surrounding media [13, 14]. Although we currently cannot measure the surface plasmon resonance energy of our nanoparticles we are confident that with 400 nm we excite the rather broad plasmon resonance [25] while with 267 nm we are probably too far off resonance. For Na clusters on LiF it has also been shown that the surface plasmon can be efficiently excited by an ultrashort laser pulse not fully in resonance with the plasmon line [26]. The high photoelectron yield at 400 nm is therefore due to the resonant excitation of the surface plasmon in the Ag nanoparticles and the subsequent decay of this collective excitation into single-particle excitations.

Time-resolved 2PPES often contributes information essential for understanding the underlying excitation and relaxation mechanisms. With this method we may gain insight into the carrier relaxation mechanisms relevant for small metal nanoparticles, in order to understand for example their catalytic properties. Here we present the first results of two-color 2PPES performed with Ag nanoparticles on a HOPG surface (Fig. 9). The pump–probe spectra recorded on pure HOPG and on HOPG covered with Ag nanoparticles are evidently different. The signal from pure HOPG reveals only the very fast relaxation processes at an intermediate state energy of 1.7 eV that corresponds to 2.05 eV kinetic electron energy (Fig. 7). In contrast, slow relaxation processes for negative as well as positive pump–probe delay are present in the signal from the Ag nanoparticles.

From this observation we can give a preliminary explanation and a tentative assignment for the observed time constant. Since the 400 nm pulse acts as probe pulse at positive delay time the corresponding pump–probe signal reveals the electronic relaxation in the Ag nanoparticles. The relaxation time of 2 ps observed for positive pump–probe delay is typ-

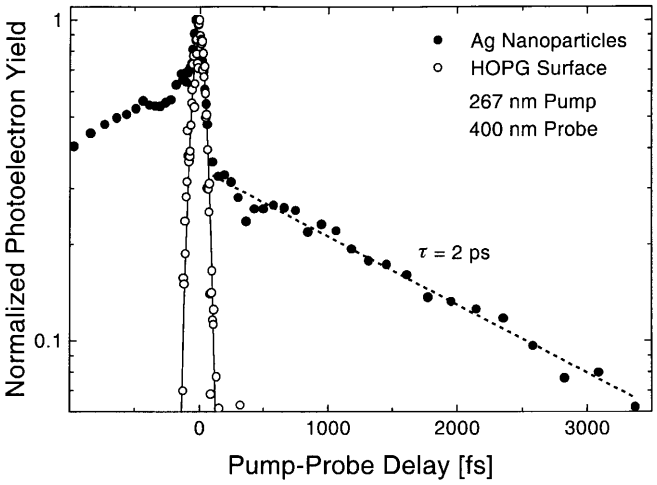


**Fig. 9.** Two-color pump–probe spectra from pure HOPG (*open symbols*) and from HOPG covered with Ag nanoparticles (*closed symbols*) recorded at 2.05 eV kinetic electron energy. The slope at positive delay was fitted by a single exponential decay

ical for the cooling of a hot electron gas due to electron phonon coupling [1] and might therefore reflect this process in the Ag nanoparticles. The reason why the relaxation at an intermediate state energy 3.3 eV above the Fermi level is so slow is not yet understood. For negative delay the 267 nm pulse probes the total surface. The deviation in the relaxation behavior from that of the pure HOPG surface might therefore be explained by a charge transfer from the nanoparticles to the HOPG or by the fact that only the excitations in the nanoparticles give rise to a pump–probe signal. If the latter explanation is correct, the initial fast process might reflect the energy relaxation of the hot carriers due to electron–electron interaction.

## Summary

We have presented two-color time-resolved 2PPES measurements on HOPG and on Ag nanoparticles on HOPG. The multiphoton photoemission spectra obtained at 400 nm (3.1 eV) and 267 nm (4.65 eV) are in good agreement with what is known about the band structure of graphite. 2PPES on pure HOPG reveals a surface state about 3.6 eV above the Fermi level. The existence of a state or band at this energy was already known from IPES and TCS, but its assignment remained controversial. The long lifetime of 60 fs seen in the time-resolved 2PPES of this state now proves that it must be an image potential state.

The investigation of the hot carrier relaxation in HOPG revealed a discrepancy between the observed pump–probe spectra and simple rate equation model calculations. We attribute this to the presence of feeding of the intermediate states. We therefore question the electron–plasmon interaction as the underlying relaxation mechanism in HOPG as proposed under the assumption of negligible feeding by Xu et al. [5]. We conclude that a more refined model and experiments at different photon energies are required to identify the physical mechanisms for hot carrier relaxation in HOPG.

The observed strong two-photon photoemission from Ag nanoparticles grown on HOPG at 400 nm excitation is attributed to the surface plasmon excitation and its subsequent decay into single-particle excitations. Time-resolved 2PPES reveals information on the carrier relaxation dynamics in a confined electron gas system and in future experiments will allow the investigation of the surface plasmon decay channels in Ag nanoparticles.

*Acknowledgements.* Finally we would like to thank H. Hövel for his kind advice concerning the preparation of metallic nanoparticles on HOPG.

## References

1. W.S. Fann, R. Storz, H.W.K. Tom, J. Bokor: Phys. Rev. Lett. **68**, 2834 (1992)
2. C.A. Schmuttenmaer, M. Aeschlimann, H.E. Elsayed-Ali, R.J.D. Miller, D. Mantell, J. Cao, Y. Gao: Phys. Rev. B **50**, 8957 (1994)
3. E. Knoesel, A. Hotzel, M. Wolf: Phys. Rev. B **57**, 12 812 (1998)
4. H. Petek, S. Ogawa: Prog. Surf. Sci. **56**, 239 (1997)
5. S. Xu, J. Cao, C.C. Miller, D.A. Mantell, R.J.D. Miller, Y. Gao: Phys. Rev. Lett. **76**, 483 (1996)
6. D. Pines, P. Nozieres: *The Theory of Quantum Liquids* (Benjamin, New York 1966)
7. L. Zheng, S. Das Sharma: Phys. Rev. Lett. **77**, 1410 (1997)
8. Th. Fauster, F.J. Himpsel, J.E. Fischer, E.W. Plummer: Phys. Rev. Lett. **51**, 430 (1983)
9. I. Schäfer, M. Schlüter, M. Skibowski: Phys. Rev. B **35**, 7663 (1987)
10. R. Claessen, H. Carstensen, M. Skibowski: Phys. Rev. B **38**, 12 582 (1988)
11. J.C. Boettger: Phys. Rev. B **55**, 11 202 (1997)
12. C.R. Henry: Surf. Sci. Rep. **31**, 231 (1998)
13. U. Kreibig M. Vollmer: *Optical Properties of Metal Clusters*, Springer Ser. Mater. Sci. **25** (1995)
14. H. Hövel, A. Hilger, I. Nusch, U. Kreibig: Z. Phys. D **42**, 203 (1997)
15. H. Hövel, Th. Becker, A. Bettac, B. Reihl, M. Tschudy, E.J. Williams: J. Appl. Phys. **81**, 154 (1997)
16. C.A. Ullrich, P.-G. Reinhard, E. Suraud: Phys. Rev. A **57**, 1938 (1998)
17. U. Busolt, E. Cottancin, H. Röhr, L. Socaciu, T. Leisner, L. Wöste: Appl. Phys. B **68**, 453 (1999)
18. MaTecK, Material-Technologie & Kristalle GmbH, Jülich, Germany
19. B. Reihl, J.K. Gimzewski, J.M. Nicholls, E. Tosatti: Phys. Rev. B **33**, 5770 (1986)
20. M. Posternak, A. Baldereschi, A.J. Fremann, E. Wimmer: Phys. Rev. Lett. **52**, 863 (1984)
21. T. Hertel, E. Knoesel, M. Wolf, G. Ertl: Phys. Rev. Lett. **76**, 535 (1996)
22. K. Ertel, J. Lehmann, M. Merschdorf, W. Pfeiffer, A. Thon, S. Voll, G. Gerber: To be published
23. D. Straub, F.J. Himpsel: Phys. Rev. B **33**, 2256 (1986)
24. K. Ertel: Diploma thesis, University of Würzburg (1998)
25. D. Steinmüller-Nethl, R.A. Höpfel, E. Gornik, A. Leitner, F.R. Aussenegg: Phys. Rev. Lett. **68**, 389 (1992)
26. M. Simon, F. Träger, A. Assion, B. Lang, S. Voll, G. Gerber: Chem. Phys. Lett. **296**, 579 (1998)